이 학 석 사 학 위 논 문

M3 인산화 부위가 PIN-FORMED 옥신수송체의 세포 내 수송 및 애기장대의 발달에 미치는 영향

The M3 Phosphorylation Region of PIN-FORMEDs Plays for their Polarity and Biological Roles in *Arabidopsis*

2016년 8월

서 울 대 학 교 대 학 원

생 명 과 학 부

기 대 은

Abstract

Asymmetrically localized PIN-FORMED (PIN) auxin efflux carriers play an important role in regulating directional intercellular auxin movement and thus generating local auxin gradients. The polar localization of PINs is tightly controlled by phosphorylation in the central hydrophilic loop (HL) of PINs. The importance of M3 phosphorylation site, which locates in evolutionarily conserved RKSNASRRSF(/L) and TPRPSNL motifs of the HL, has been reported for PIN3. Here, we analyzed the conserved role of the M3 phosphorylation site of PIN1 and PIN7. Phosphorylation-defective mutations of five phosphorylatable residues (Ser/Thr to Ala or Gly) in the M3 site of PIN1-HL changed its subcellular polarity and caused defects in PIN1-mediated biological functions such as floral organ formation, root growth and leaf phyllotaxy. The M3 phosphorylation-defective mutants of PIN7 impaired its proper subcellular trafficking in root

columella cells, which then disrupted normal root gravitropism. Our data indicate that the M3 phosphorylation site is functionally conserved among long PINs and plays important roles for their subcellular trafficking, auxin distribution, and auxin-mediated developmental processes.

.....

Keywords: Auxin, Auxin transport, Hydrophilic loop (of PINs), Phosphorylation, PIN-FORMED (PIN), Protein trafficking

Student ID.: 2014-21269

CONTENTS

ABSTRACT i

CONTENT iii

LIST OF FIGURES v

ABBREVIATIONS vi

1 INTRODUCTION 1

2 MATERIALS AND METHODS 9

2.1 Plant materials and growth conditions 9

2.2 Observation of biological parameters 10

2.3 Transgene constructs 10

2.4 Accession Numbers 12

2.5 *In vitro* phosphorylation assay 13

3 RESULTS 15

3.1 Proper PIN1 trafficking and polarity requires the M3 phosphorylation site 15

3.2 The M3 phosphorylation site is required for PIN1-mediated plant development 21

3.3 In vitro analysis revealed the difference of phosphorylation level in M3 and 3m1 mutation 29

3.4 Gravity-induced PIN7 relocalization and its resulting gravitropism requires phosphorylation of M3 region 33

4 DISCUSSION 38

5 LITERATURES CITED 43

6 ABSTRACT IN KOREAN 50

LIST OF FIGURES

FIGURE 1. Five conserved S/T residues in the M3 region among long-looped PIN orthologues.

FIGURE 2. Effects of M3 and 3m1 mutations on the polarity and trafficking of PIN1.

FIGURE 3. Effect of M3 or 3m1 mutation of PIN1 on seedling development.

FIGURE 4. Effect of M3 or 3m1 mutation of PIN1 on phyllotaxis of vegetative leaves.

FIGURE 5. Effect of M3 or 3m1 mutation of PIN1 on reproductive development.

FIGURE 6. *In vitro* phosphorylation assay of the hydrophilic loop (HL) of PIN1 and PIN7.

FIGURE 7. Effect of M3 mutation on PIN7 trafficking and root gravitropism.

Table 1. Primer list.

ABBREVIATIONS

ATP	Adenosine tri-phosphate
BFA	Brefeldin A
CHX	Cycloheximide
EDTA	Ethylenediaminetetraacetic acid
EGTA	Ethylene glycol tetraacetic acid
E7	*EXPANSIN A7*
GFP	Green Fluorescence Protein
IPTG	Isopropyl b-D-1-thiogalactopyranoside
$MgCl_2$	Magnesium chloride
MS	Murashige-Skoog
PCR	Polymerase chain reaction
PID	PINOID
PIN	PIN-FORMED Protein
PM	Plasma Membrane
PP2A	Protein phosphatase 2A
WT	Wild type

1. Introduction

The plant hormone auxin is implicated in diverse processes in plant growth and development. Differential distribution of auxin within plant tissues is essential for auxin-mediated developmental processes (Grunewald and Friml, 2010; Ganguly et al., 2012b). Local auxin gradients are mostly mediated by auxin transporter proteins, of which PIN-FORMED (PIN) auxin efflux carriers are the key regulators as their asymmetrical localization at the plasma membrane (PM) (Wiśniewska et al., 2006). The directional intercellular transport of auxin subsequently results in many aspects of auxin-related development, involving embryonic axis formation, organ formation, tissue patterning, and tropic growth (Grunewald and Friml, 2010).

The Arabidopsis genome encodes eight PIN proteins that can be classified into two subgroups by their size of central hydrophilic loop (HL) domains. PIN1 to PIN4, PIN6, and PIN7 have a long HL (298–377 residues; long PINs), whereas PIN5 and PIN8 have a relatively short HL (27–46 residues; short PINs) (Křeček et al., 2009; Ganguly et al., 2012b). While short PINs localize to either internal compartments or PM depending on PIN and cell type, long PINs predominantly localize to the PM (Ganguly et al., 2010; 2014).

Conversely, distinct subcellular polarity caused by asymmetrical localization of long PINs in PM determines the direction of cell–to–cell auxin transport (Wiśniewska et al., 2006; Grunewald and Friml, 2010). In response to developmental and environmental cues, the subcellular PIN polarity can be changed dynamically (Friml et al., 2002b; Friml et al., 2003; Benkova et al., 2003).

PIN proteins show different subcellular localization depending on the cell type and the PIN proteins (Wiśniewska et al., 2006; Ganguly et al., 2014). PIN1, −3, −4, and −7 are typically localize at the basal plasma membrane toward the root tip in Arabidopsis root (Friml et al., 2002a, 2002b; Blilou et al., 2005). In contrast, PIN2 protein localizes apically (towards the shoot) in root epidermal, elongating cortex and lateral root cap cells and basally (towards the root) in young cortex cells (Muller et al., 1998). In root columella cells where PIN3 and PIN7 are expressed, PIN3 and PIN7 proteins show flexible PIN polarity changes in response to gravity stimulation (Friml et al., 2002b; Kleine−Vehn et al., 2010). Although the direct role of transmembrane of PINs has not been reported, there are several molecular cues in the hydrophilic loop of long PINs in regulation of intracellular trafficking of PIN proteins (Ganguly et al., 2013).

In PIN trafficking and polarity, PIN phosphorylation and dephosphorylation play a decisive role (Ganguly et al., 2012b). AGC kinase family from Arabidopsis thaliana has been reported to play an important role in phosphorylation of PIN efflux carriers and of ABC transporters and subsequently the auxin transport-dependent growth (Zhang and McCormick, 2008; Ganguly et al., 2012b; Barbosa and Schwechheimer, 2014). Among the AGCVIII kinases, Serine/Threonine(S/T) kinase PINOID (PID) and protein phosphatase 2A (PP2A) have been implicated to regulate PIN polar targeting and consequently result in plant growth and development (Bennett et al., 1995., Friml et al., 2004, Michniewicz et al., 2007, Lee and Cho, 2006). Importantly, the antagonistic action of PID and PP2A directly targets to the hydrophilic loop of PINs (PIN-HL) and regulate the subcellular polarity of PIN proteins (Friml et al., 2004, Michniewicz et al., 2007). The PIN-specific and cell type-specific localization of PIN proteins can be caused by different expression

levels of PID and PP2A in the cell type and diverse phosphorylation sites of each PINs (Kleine-Vehn and Friml, 2008). As a consequence, PIN-HL phosphorylation by PID or related kinase modulate subcellular polarity and biological function (Huang et al., 2010; Dhonukshe et al., 2010; Zhang et al., 2010, Ganguly et al., 2012a).

The evolutionary conserved TPRXS(N/S) motifs within the PIN-HL have been studied that the Serine residue in this motif is phosphorylated by PINOID (PID) kinase (Huang et al., 2010; Dhonukshe et al., 2010). Single or multiple mutation of these three TPRXS(N/S) motifs (S1, S2, S3) in PIN1-HL showed PIN1-mediated defect in subcellular localization and its biological functions (Huang et al., 2010). Recent study also showed that two phosphosites (S4, S5) are conserved in PIN1 (S4 only), PIN3, PIN4 and PIN7 which is activated by D6PK (Zourelidou et al., 2014).

Also, The M3 phosphorylation-defective mutation which includes serine/threonine double mutant (to Alanine) of the first TPRXS(N/S) motif (2m3; T222A-S226G) with triple mutant of RKSNASRRSF(/L) (3m1; S209A- S212A-S215G) was reported that this M3 site play an important role in PIN polarity and related biological function (Ganguly et al., 2012a; Sasayama et al., 2013). Phosphorylation-defective mutation of M3 site (M3PIN3) under root hair cell specific EXPANSIN A7 promoter (Cho and Cosgrove, 2002; Kim et al., 2006; Lin et al., 2011) and its own promoter (proPIN3) showed clear defect in normal PIN3 polarization and PIN3 mediated auxin distribution (Ganguly et al., 2012a). Accordingly, in planta and in vitro phosphorylation analysis proved that the phosphorylation level of M3PIN3 compared to wild-type was lowered by PID kinase (Ganguly et al., 2012a). Because the M3 phosphorylation site are well conserved among the all long PINs, the M3 phosphorylation sites of PIN1, -2 and -7 have been studied

under the E7 promoter (Sasayama et al., 2013). Under root hair cell specific E7 promoter, the PM targeting of the PIN1 and −7 was impaired in M3 phosphorylation−defective mutants in the Arabidopsis root hair cell and the cellular level of PIN2 was extremely decreased in M3 mutants (Sasayama et al., 2013).

Among the 6 putative phosphorylation site (M1−M6PIN3) in PIN3−HL, the M3PIN3 mutant revealed distinct defect in subcellular localization and biological function (Ganguly et al., 2012a). Also, our previous study showed the functional conservation of M3 motif in Arabidopsis root hair cells (Sasayama et al., 2013). In this study, we generate M3 and 3m1(triple mutations for S209A -S212A−S215G) mutation lines of PIN1 and −7 under its own promoter (proPIN1 and proPIN7) to study the native role of M3 phosphorylation site in their own expression domain. We demonstrate the functional conservation of M3 phosphorylation among the all PINs and confirm its importance in

PIN trafficking, auxin-regulated plant growth and plant development.

2. Materials and Methods

2.1 Plant Materials and Growth Conditions

Arabidopsis thaliana (Columbia ecotype) was used as the wild-type plant in this study. *Arabidopsis* plants were transformed using *Agrobacterium tumefaciens* strain C58C1 (pMP90) (Bechtold and Pelletier, 1998). All seeds were cold treated (4° C) for 3 days and germinated at 22° C under 16-h-light/8-h-dark photoperiod. All the seeds were grown on agarose plates containing 4.3 g/L Murashige and Skoog (MS) nutrient mix (Sigma-Aldrich), 1% sucrose, 0.5 g/L MES (pH 5.7), KOH, and 0.8% agarose. Transformed plants were selected on hygromycin-containing plates (30 μg/mL).

2.2 Observation of biological parameters

For the root gravitropism assay, 3-day-old seedlings grown vertically in the light were turned 90° for the indicated period of time (2-10 h) in the dark condition before observing root bending. Leaves for phyllotatic analysis were numbered in order of initiation and the angles between the numbered leaves were measured by Leica Application suite (v.2.8.1). Siliques were obtained for analyzing size and number of seeds under Leica MZFLIII dissecting microscope. At least 7 siliques were used from each plant.

2.3 Transgene constructs

The binary vector pCAMBIA 1300-NOS with modified cloning sites (Lee *et al.*, 2010) was used for transgene construction. The *ProPIN:PIN:GFP* construct were performed using *ProE7:PIN:GFP*

as templates and the primer listed in the Table 1. Site-directed mutagenesis of putative phosphorylation sites of PIN1-HL and PIN7-HL to generate *ProPIN:3m1-PIN:GFP* and *ProPIN:M3-PIN:GFP* was performed by the PCR method using *ProPIN:PIN:GFP* constructs as templates and the primers listed in Table 1. Those phosphor-mutated *PIN:GFP* fragments were cloned into the binary vector containing the ProPIN fragment.

For Escherichia coli expression of PIN-HL protein for the *in vitro* phosphorylation assay, the PIN-HL part was amplified from Arabidopsis cDNA and cloned into the *pGEX-4T-1* vector (GE Healthcare, Incho, Korea) for fusion with glutathione S-transferase (GST) at the N-terminus. Full-length PINOID (PID) (Ganguly et al., 2012a) was used for *in vitro* kinase assay. All constructs were confirmed by nucleotide sequencing, and at least 5 independent transgenic lines were analyzed for each construct.

2.4 Microscopic observations

Measurement of fluorescent reporter and organelle markers were conducted as described previously (Ganguly et al., 2010; Ganguly et al., 2012a). For BFA study, seedling were pretreated with cycloheximide (CHX, 50 μM) for 30 min and followed by brefeldin A (BFA, 25 μM) for 30 min. Wortmannin (20 μM) was treated to the seedlings before observation as described in the figures. The quantification of PM-localized *PIN:GFP* signals was performed using the histogram of Adobe Photoshop 6.0 software.

For gravitropic polarity change experiments, 4-day-old seedlings were transferred to slide containing half strength MS medium and grown vertically in the dark condition. Gravity stimulation was applied for indicated time by positioning plate and subsequently analyzed with confocal microscopy.

2.5 *In vitro* phosphorylation assay

Glutathione S-transferase-fused kinases (PID) and substrates (wild-type and mutated PIN-HL) were expressed in E. coli BL21DE3 cells by induction for 3 h with 1 mM isopropyl β-D-1-thiogalactopyranoside at 28° C, and the cells were harvested by 10 min 4300 rpm centrifugation. After that, the cells were lysed with B-PER bacterial protein extraction reagent (Thermo Scientific, Seoul, Korea) with the Halt protease inhibitor complex(Santa cruz), and purified using GST bind agarose resin (Elpis biotech). For *in vitro* phosphorylation assays, 1 μg of kinase and substrate proteins was mixed in 30 μl kinase buffer (25 mM Tris-HCl pH 7.5, 1 mM DTT, 5 mM $MgCl_2$, 100 uM sodium orthovanadate, 30 mM β-glycerophosphate) and 1 μCi [γ-32P] ATP for 1hour at 30° C.

Table 1. Primer list

subject	Template	Primer Name	Sequence (5' to 3')
PIN1,7 mutation		E7 5'-tDNA	TGA AAA TCC CCT CTA TAT AAG ATT GTC TC
		mGFP4R118	CCG TAT GTT GCA TCA CCT TCA CCC T
PIN1 promoter	ProE7:PIN1:GFP	PIN1PR-Hd-F	GTT TAA GCT TCC ATA ACC ATA AGT CAA GCC GTG C
		PIN1PR-Sl-R	GTT TGT CGA CCT TTT GTT CGC CGG AGA AGA GAG
PIN7 promoter	ProE7:PIN7:GFP	PIN7PR-Hd-F1	GTT TAA GCT TCT CTC TTT CTT CAG TGA TG
		PIN7PR-Sl-R	TTA GTC GAC ATT GTT GTT CGC CGG AGT GG
PIN1-3m1 mutation	ProE7:PIN1:GFP	PIN1 M3A-R1	TTG AGC CCT TCT CGA GTA AAT ATC AGA CCT TGC AGC ATT AGC ACG ACG AAC
PIN1-M3 mutation	ProE7:PIN1-3m1:GFP	PIN1 M31-R2	GGT TAG ATT CGC AGG TCT AGG TGC CGC AGA TAA
PIN7-3m1 mutation	ProE7:PIN7:GFP	PIN7-M3A-R1	ACC ACC GTA AAA AGC TCT CCG AGC AGC GTT TGC TTT TCT CAC
PIN7-M3 mutation	ProE7:PIN7-3m1:GFP	PIN7-M3R2	GGT GAG ATT AGC CGG ACG AGG AGC CAT ATT AGT

3. Results

3.1 Proper PIN1 trafficking and polarity requires the M3 phosphorylation site

In the root, PIN1 is mainly localized at the basal PM of vascular cells and basal and inner lateral side in pericycle and endodermal cells (Gälweiler et al., 1998). In order to study the effect of M3 and 3m1 phosphorylation sites on subcellular localization of PIN1, wild-type PIN1 and mutated PIN1 at the M3 or 3m1 region (M3PIN1 or 3m1PIN1; Figure 1) of the HL domain were expressed under its own promoter (*ProPIN1*) in the *pin1* mutant background. For each construct, at least 5 independent transgenic lines were observed by a confocal microscope.

In vascular cells, wild-type PIN1, as expected, predominantly localized to the basal PM, whereas the basal

localization of M3PIN1 was disturbed so as for the mutant PIN1 to be more localized to lateral sides than wild-type PIN1 (Figure 2A). Moreover, M3PIN1 more tended to be internalized than wild-type PIN1. Statistical analysis obviously revealed the defects of M3PIN1 and 3m1PIN1 in basal localization by showing considerably decreased ratio of apical/basal to lateral localization (Figure 2B, C). In endodermal cells, while wild-type PIN1 localized predominantly in basal and inner lateral sides, mutation of M3 or 3m1 disturbed this polarity by delivering these mutant PINs to the outer lateral PM (Figure 2D-F). These results indicate that the subcellular PIN1 polarity requires the M3 phosphorylation sites.

When roots were treated with the PIN-recycling inhibitor brefeldin A (BFA), both wild-type PIN1 and M3PIN1 formed internal BFA compartments (Figure 2G), suggesting that M3PIN1 is localized to the PM and properly recycles like wild-type PIN1.

In previous study, ectopic cell division was observed in the M3PIN3-expressing root pericycle (Ganguly et al., 2012a). M3PIN1 and 3m1PIN1 also caused a considerable increase of ectopic cell division in the pericycle (Figure 2H, I). It is likely that disruption of PIN subcellular polarity generally causes ectopic cell division probably by interfering local auxin concentration gradients.

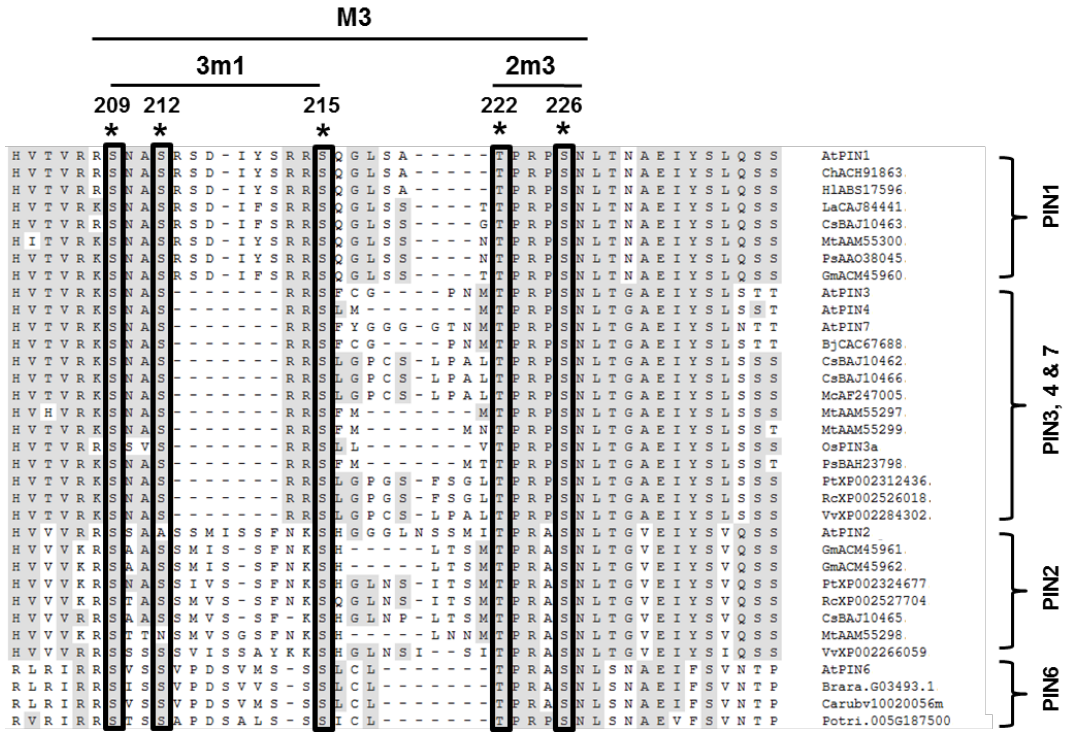

Figure 1. Five conserved S/T residues in the M3 region among long-looped PIN orthologues.

Species names: Bj, Brassica juncea; Ch, Cardamine hirsuta; Cs, Cucumis sativus; Gm, Glycine max; Hl, Humulus lupulus; La, Lupinus albus; Mc, Momordica charantia; Mt, Medicago truncatula; Os, Oryza sativa; Ps, Pisum sativum; Pt, Populus trichocarpa; Rc, Ricinus communis; Vv, Vitis vinifera.

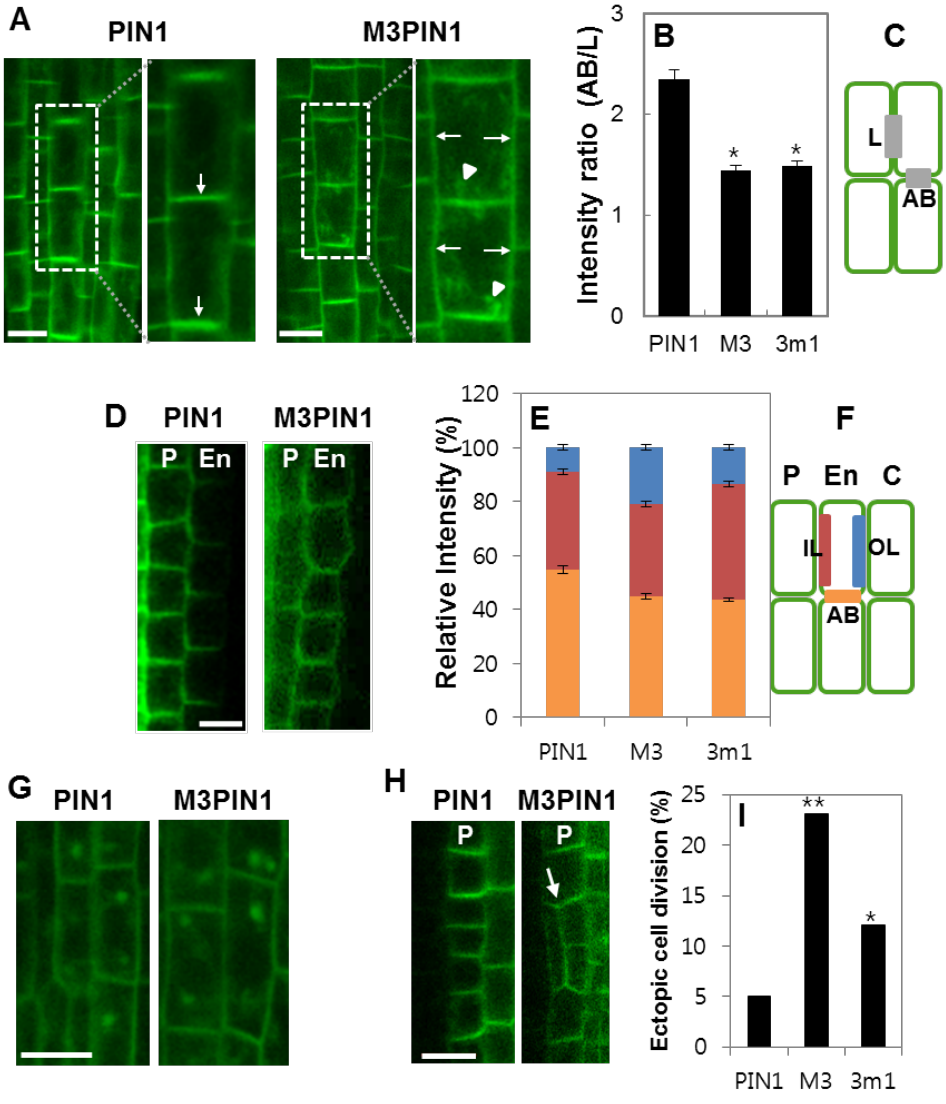
A
PIN1
M3PIN1
B
Intensity ratio (AB/L)
3
2
1
0
*
*
PIN1
M3
3m1
C
L
AB
D
PIN1
M3PIN1
P
En
P
En
E
Relative Intensity (%)
120
100
80
60
40
20
0
PIN1
M3
3m1
F
P
En
C
IL
OL
AB
G
PIN1
M3PIN1
H
PIN1
M3PIN1
P
P
I
Ectopic cell division (%)
25
20
15
10
5
0
**
*
PIN1
M3
3m1

FIGURE 2. Effects of M3 and 3m1 mutations on the polarity and trafficking of PIN1

(A) Representative confocal images of PIN1 (*ProPIN1:PIN1:GFP*) and M3PIN1 (*ProPIN1:M3PIN1:GFP*) in root vasculature cells. Arrows indicate basally intensified and laterally depolarized localization of PIN1 and M3PIN1, respectively. Arrowheads indicate internalized compartments of M3PIN1. Bar=10 μm.
(B, C) Quantification of the PIN polarity shown in (A). The fluorescence ratio of apical and basal (AB)/lateral (L) membranes sides (grey bars in C) of PIN1, M3PIN1, and 3m1PIN1 (*ProPIN1:3m1PIN1:GFP*). Data represent means±SE (n=24-27 cells from 7-8 roots for each construct). Asterisks indicate that differences are significant from the PIN1 control ($P<0.0001$).
(D) Representative confocal images showing the subcellular localization of PIN1 and M3PIN1 in pericycle (P) and endodermis (En) cells of the root. Bar=10 μm.
(E, F) Quantification of the PIN polarity in the endodermis shown in (D). The fluorescence ratio of outer lateral (OL in blue), inner lateral (IL in red), and apical and basal (AB in orange) membrane as shown in (C) was estimated with wild type and mutant PIN1 lines (P, pericycle; En, endodermis; C, cortex). Data represent means±SE (n=25 cells from 8-9 roots for each construct).
(G) Representative confocal images of BFA body in PIN1- and M3PIN1-expressing root stele under its own promoter. Bar=10 μm.
(H) Representative confocal images of ectopic cell division in the wild type or mutant PIN1-expressing root pericycle (P). Arrow indicates ectopic cell division region. Bar=10 μm.
(I) Ratio of seedlings showing ectopic cell division in pericycle and endodermis cells (n=18 seedlings each). Data are significantly different from PIN1 value at $P<0.05$(*) and $P<0.0001$(**).

3.2 The M3 phosphorylation site is required for PIN1-mediated plant development

It is conceivable that polarity changes of PIN1 affect auxin-dependent plant growth and development. The *pin1* mutant shows structural abnormalities in inflorescence axes, flowers and leaves (Okada et al., 1991). To investigate the biological roles of M3 and 3m1 phosphorylation sites, phenotypes of *pin1* complemented M3PIN1 and 3m1PIN1 were analyzed.

During embryo development, the loss of PIN1 causes aberrant cotyledon morphogenesis such as single, multiple, and fused cotyledons (Figure 3A). In cotyledon analysis, F1 progeny seedlings of self-fertilized hemizygous *pin1* mutant were used because almost all of the M3PIN1 mutant could not produce seeds for next generation. In contrast with *pin1* complemented PIN1-GFP, M3PIN1 and 3m1PIN1 partially rescued the *pin1* cotyledon

defects (Figure 3B). Surprisingly, the number of seedling with fused cotyledon increased in 3m1PIN1 complemented plants to about 3.3% (n=485) (Figure 3A, B). Also, some severe defects such as reduced or no cotyledons were observed in both 3m1PIN1 and M3PIN1.

Because PIN1 is highly linked to the organ initiation and phyllotaxis (Okada et al., 1991; Reinhardt et al., 2003; Prasad et al., 2011), we examined rosette leaf phyllotaxis of M3PIN1 and 3m1PIN1 complemented lines first. In the M3PIN1 and 3m1PIN1, the divergence of leaf angle deviated from the canonical 137.5° value and the rosette leaf phyllotaxis spread out from the 137.5° (Figure 4A, B). This data supported that the M3PIN1 and 3m1PIN1 could not completely complement the wild-type PIN1. In the early stage of bolting, M3PIN1 showed pin-like bolting similar with *pin1* (Figure 5C). Subsequently, we observed the early abortion of primary stem in M3PIN1 and increased lateral

shoot (Figure 5A, D). Consistent with this data, the average height of 6-week old plants of M3PIN1 was shorter than that of wild type.

The M3PIN1 and 3m1PIN1 mutants produced aberrant or no silique (Figure 5D). Therefore, we counted siliques with over 1cm and seeds in the siliques. The wild-type plants generally produced over 1.5cm siliques, otherwise M3 mutants showed severe defect in silique development (Figure 5E). The 3m1PIN1 mutant occasionally produced defective flowers to produce seeds (Figure 5D, E). In contrast to the PIN1 complementation lines, M3PIN1 and 3m1PIN1 mutant lines showed decreased number of silique (Figure 5E). 3 out of 5 lines of M3PIN1 produced no silique over 1cm at all, and 3m1PIN1 mutant lines produced decreased number of silique over 1cm (Figure 5E). Consistently, defect of silique development in M3 and 3m1 mutant led to reduced number of seeds per silique. Compared to the number of

seeds per silique of Wild type (~40.9 seeds/silique), *pin1* complemented with M3PIN1 (M3, *ProPIN1:M3PIN1:GFP*) and 3m1PIN1 (3m1, *ProPIN1:3m1PIN1:GFP*) had only 4.6 and 27.6 seeds per silique, respectively (Figure 5F, G).

These results suggest that phosphorylation in the M3 region of PIN1-HL is important in plant development such as leaf phyllotaxis, seedling formation, flowering and silique development.

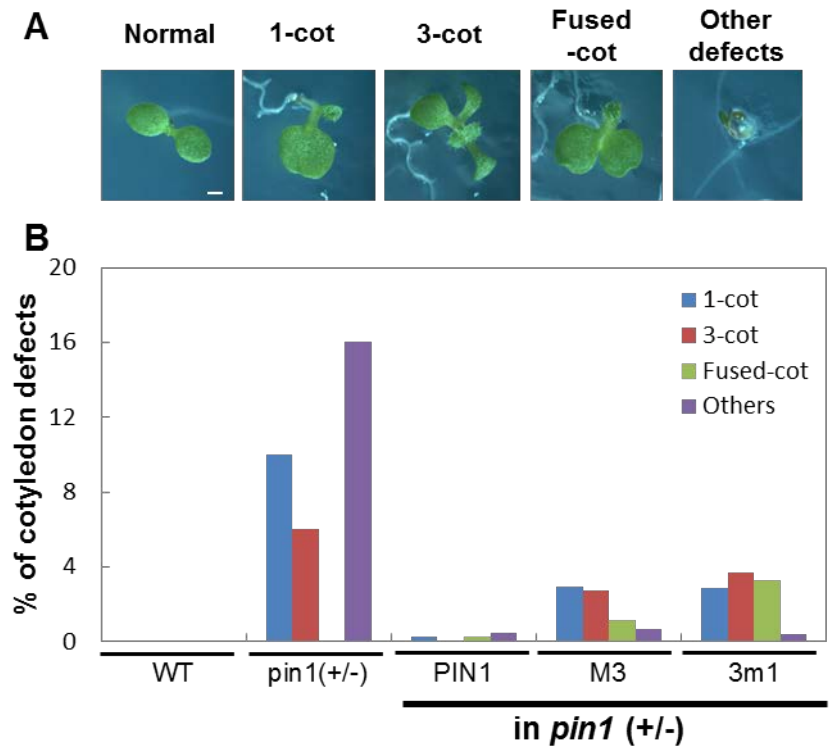

FIGURE 3. Effect of M3 or 3m1 mutation of PIN1 on seedling development.

(A) Six-day-old seedlings showing cotyledon defects by PIN1 mutations. Bar=0.5 mm.

(B) Quantification of cotyledon defects shown in (A). All the segregated F1 progeny seedlings of self-fertilized hemizygous *pin1* (+/-) mutant background were observed for *pin1* and *pin1* with PIN1 (*ProPIN1:PIN1:GFP*), M3PIN1 (M3, *ProPIN1:M3PIN1:GFP*), and 3m1PIN1 (3m1, *ProPIN1:3m1PIN1:GFP*). Total 403-485 seedlings from 7-8 independent lines per construct were observed. WT, wild type.

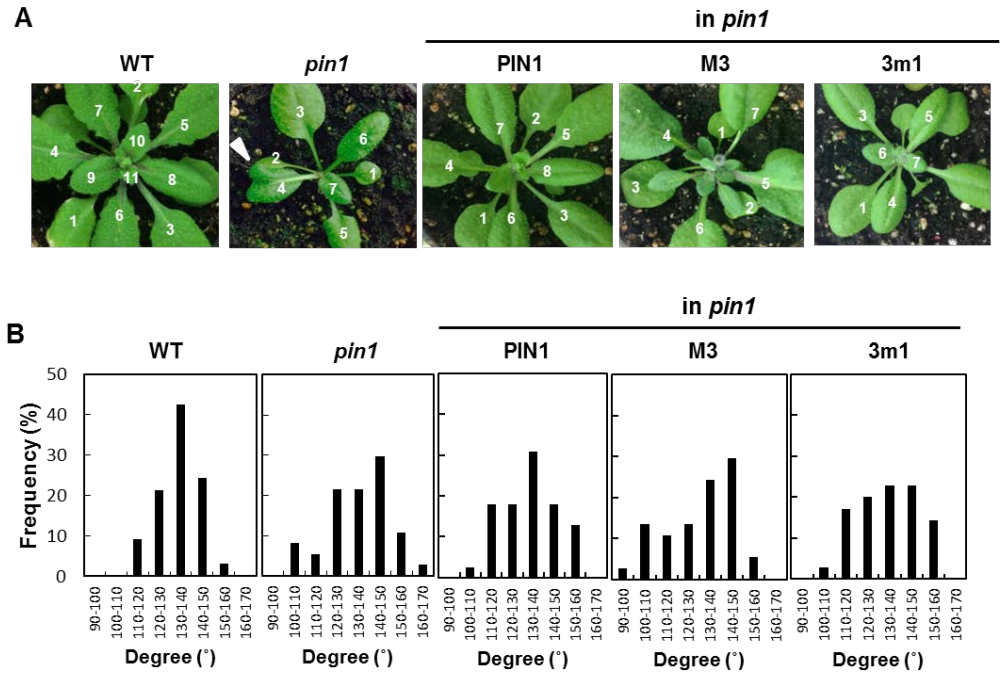

FIGURE 4. Effect of M3 or 3m1 mutation of PIN1 on phyllotaxis of vegetative leaves.

(A) Images of rosette leaves of wild type (WT), *pin1*, and *pin1* complemented with PIN1 (*ProPIN1:PIN1:GFP*), M3PIN1 (M3, *ProPIN1:M3PIN1:GFP*), and 3m1PIN1 (3m1, *ProPIN1:3m1PIN1:GFP*). Arrow head indicates fused leaf shown in *pin1* mutant.

(B) Distribution of leaf-emerging angles in the plants described in (A) (n=33-39 plants [in case of transgenics, from 5-7 independent lines for each construct]).

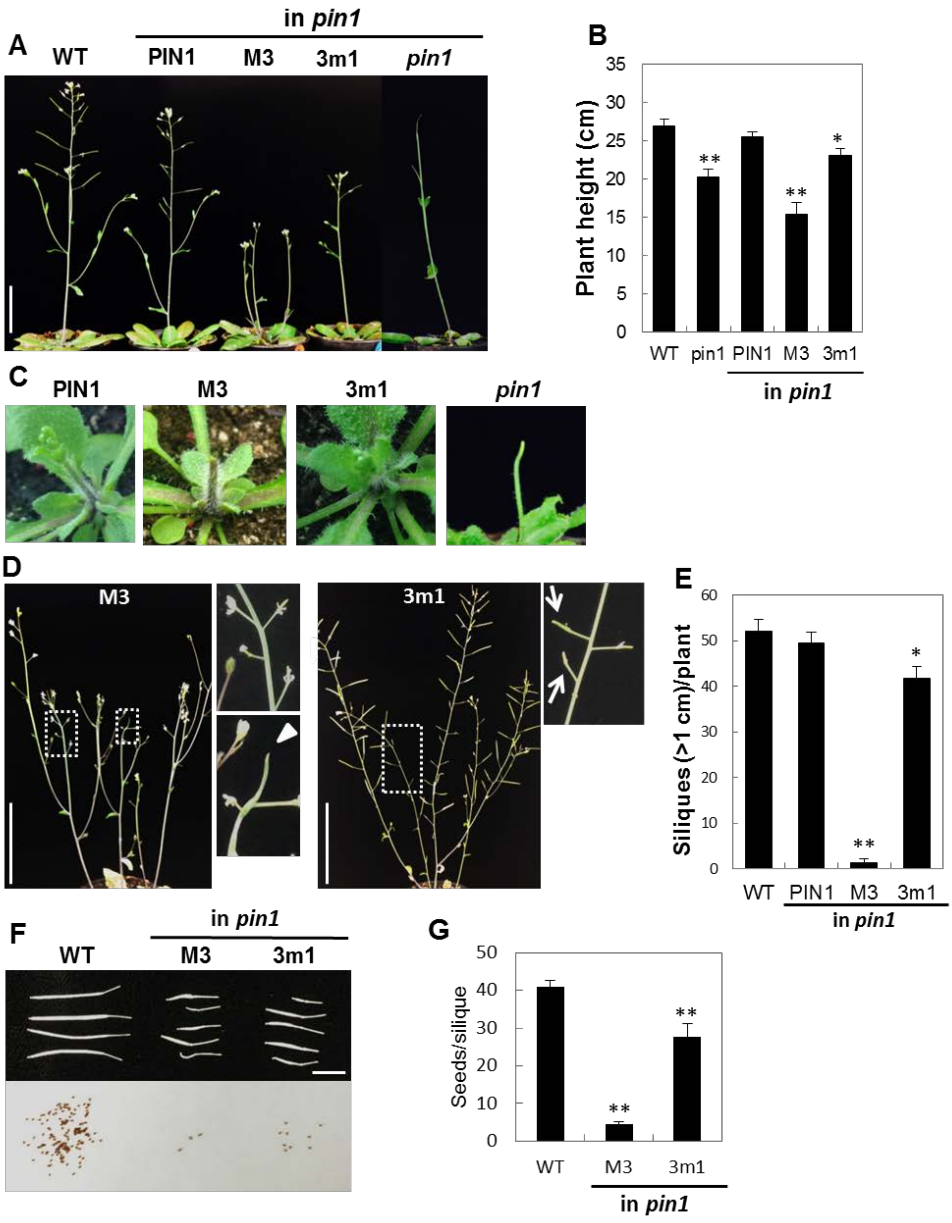
A
in pin1
WT
PIN1
M3
3m1
pin1
B
Plant height (cm)
35
30
25
20
15
10
5
0
**
**
*
WT
pin1
PIN1
M3
3m1
in pin1
C
PIN1
M3
3m1
pin1
D
M3
3m1
E
Siliques (>1 cm)/plant
60
50
40
30
20
10
0
**
*
WT
PIN1
M3
3m1
in pin1
F
in pin1
WT
M3
3m1
G
Seeds/silique
50
40
30
20
10
0
**
**
WT
M3
3m1
in pin1

FIGURE 5. Effect of M3 or 3m1 mutation of PIN1 on reproductive development.

(A) Inflorescence stems of wild-type (WT), *pin1*, and *pin1* complemented with PIN1 (*ProPIN1:PIN1:GFP*), M3PIN1(M3, *ProPIN1:M3PIN1:GFP*), and 3m1PIN1 (3m1, *ProPIN1:3m1PIN1:GFP*). Bar=5 cm.
(B) Average height of the plants in (A). Data represent means±SE (n=7-10). Data are significantly different from WT value at $P<0.05$(*) and $P<0.005$(**).
(C) Images showing early development of the inflorescence stem.
(D) Defects in reproductive organs by M3 or 3m1 mutation. Arrowhead indicates defect in the stem tip of the M3 transformant. Arrows indicate defect in siliques of 3m1 transformants.
(E) Number of silique over 1 cm in length. Data represent means±SE (n=5-8 plants). Data are significantly different from WT value at $P<0.05$(*) and $P<0.005$(**).
(F) Images of representative siliques and seeds from WT, M3 and 3m1 plants. Seeds were harvested from the siliques shown in the upper photograph. Bar=5 mm.
(G) Number of seeds per silique. Data represent means±SE (n=8-20 siliques). Data are significantly different from WT value at $P<0.005$(**).

3.3 In vitro analysis revealed the difference of phosphorylation level in M3 and 3m1 mutation

To determine the different phosphorylation level in wild-type, M3 and 3m1, we constructed glutathione S-transferase (GST)-tagged *GST:PIN-HL*, *GST:M3PIN-HL* and *GST:3m1PIN-HL* for *in vitro* kinase assay. M3 and 3m1 mutated PIN1- and PIN7-HL showed reduced phosphorylation level compared to the WT-PIN-HL by PID (Figure 6). Mutation of Ser/Thr-to-Ala in M3 site of PIN1-HL led to ~45% reduction, and 3m1 site mutation led to ~8% reduction (Figure 6A). Consistently, M3PIN7 and 3m1PIN7 phosphorylation by PID was reduced to ~44 and ~33%, respectively (Figure 6B). However, in case of PIN7 *in vitro* kinase assay, the phosphorylation level was relatively low compared with PIN1- and PIN3-HL (Figure 6B). Coincide with M3PIN3 phosphorylation analysis (Ganguly et al., 2012a), these data

suggest that the M3 site of PIN-HL is an important phosphosite for PID *in vitro*.

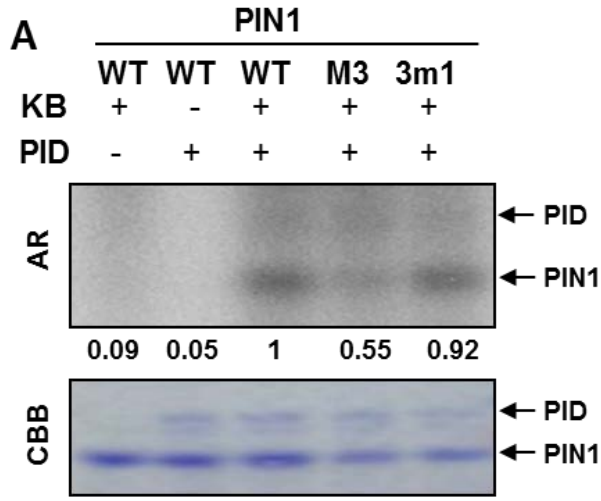
A
PIN1
WT WT WT M3 3m1
KB + - + + +
PID - + + + +
AR
PID
PIN1
0.09 0.05 1 0.55 0.92
CBB
PID
PIN1

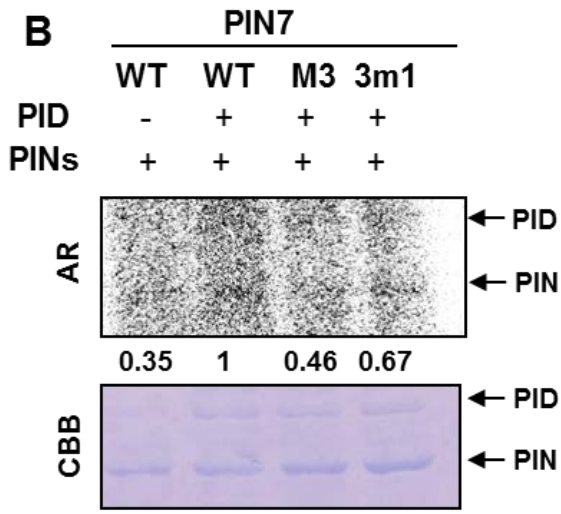
B
PIN7
WT WT M3 3m1
PID - + + +
PINs + + + +
AR
PID
PIN
0.35 1 0.46 0.67
CBB
PID
PIN

Figure 6. *In vitro* phosphorylation assay of the hydrophilic loop (HL) of PIN1 and PIN7.

(A) Autoradiogram (AR) of PIN1-HL phosphorylation assay. Wild type (WT), M3, and 3m1 PIN1-HL proteins were analyzed for phosphorylation by PID kinase using [$\gamma-^{32}$P] ATP as a phosphate source. CBB, coomassie brilliant blue-stained gel. CBB, Coomassie Brilliant Blue-stained gel. The band intensity from AR was normalized by corresponding band intensity from CBB. Percentage values represent quantified amount of band intensity relative to wild type protein.

(B) Autoradiogram (AR) of PIN7-HL phosphorylation assay. Wild type (WT), M3, and 3m1 PIN7-HL proteins were analyzed as in (A).

3.4 Gravity-induced PIN7 relocalization and its resulting gravitropism requires phosphorylation of M3 region

The PIN3 and PIN7 in columella cells redistributes upon gravity change and it causes gravitropic bending of the root (Friml et al., 2002b; Kleine-Vehn et al., 2010). The originally uniform distribution of PINs in the columella reorganizes toward the newly oriented bottom side and it leads to auxin redistribution and root bending.

In this study, because the auxin flow caused by gravity change is considered as a crucial factor for root gravitropism, the subcellular localization of phosphorylation-defective PIN7 was studied in response of gravity change. The observation of wild-type PIN7 in short gravity stimulus (15min) by 90° induced internalization of *proPIN7:PIN7-GFP* (Figure 7A). On the other

hand, M3PIN7 mutant showed reduced internalization after short gravity stimulus for PIN7 relocalization (Figure 7A). After 40min gravity stimulus by 90° rotation, the relocalization of M3PIN7 mutant partially impaired compared to wild-type PIN7 (Figure 7B). Whereas the relative lateral membrane intensity (L/B; bottom after 90° rotation) of wild-type PIN7-GFP showed about 1.5 times higher lateral membrane intensity than that of basal, M3PIN7-GFP only showed 1.02 times higher lateral membrane intensity level (Figure 7D). These findings suggest that the M3 site phosphorylation of PIN7 is important for redistribution and transcytosis of PIN7 toward the gravity change.

After the observation of gravity-induced transcytosis defect in M3PIN7 mutant in columella cells, we performed the root gravitropism measurement of M3PIN7 and 3m1PIN7 mutants in *pin7* mutant background. The *pin7* mutants exhibited root gravitropic defect as reported previously (Friml 2002b; Kleine-

Vehn et al., 2010; Figure 7D). While complementation of the *pin7* with wild-type PIN7 rescued root gravitropism, the M3PIN7 and 3m1PIN7 failed to rescue root gravitropism of *pin7* (Figure 7C). The observation of root gravitropic kinetics showed relatively slow response of M3PIN7 and 3m1PIN7 mutants compared to the wild type (Figure 7C). The—previous study of M3PIN3 also showed that the M3 site phosphorylation is required for root gravitropism and auxin redistribution by kinetics and *DR5:ER-RPF* analysis (Ganguly et al 2012a). With this PIN3 result, the defect of gravity-induced transcytosis and its resulting gravitropism defect in M3 and 3m1 transformants demonstrated that the response of gravity requires the phosphorylation in M3 region in columella cells.

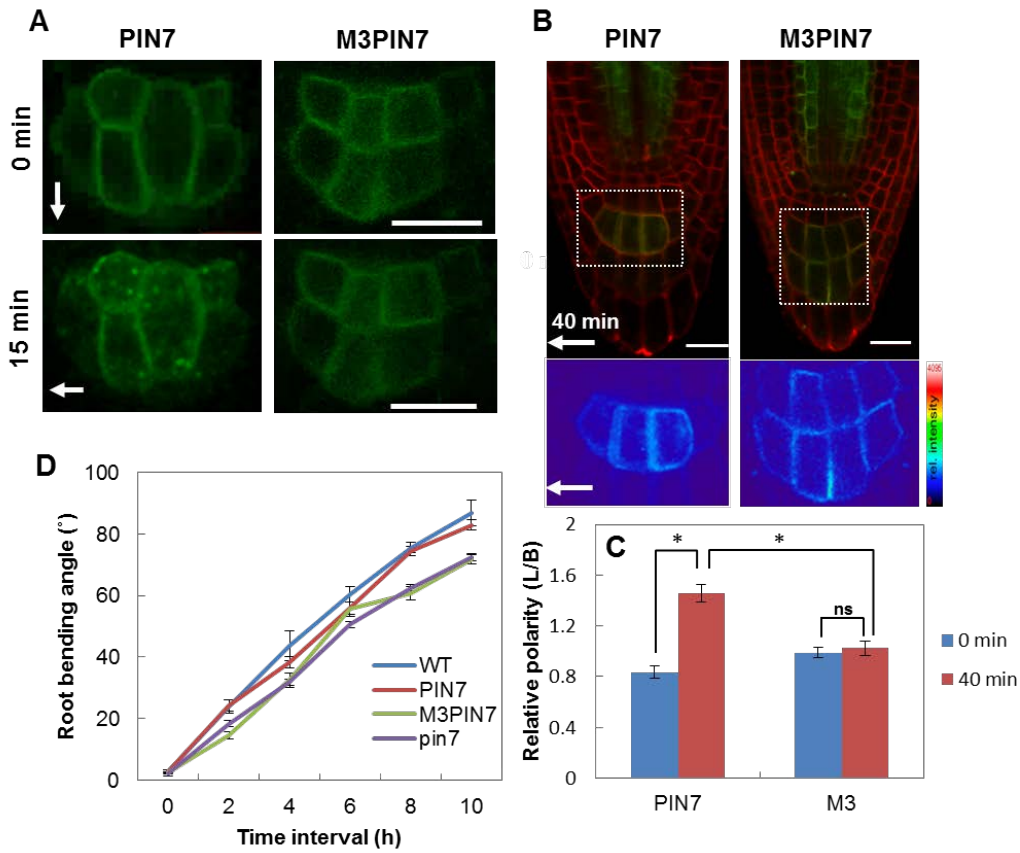
A
PIN7
M3PIN7
0 min
15 min
B
PIN7
M3PIN7
40 min
rel. intensity
C
Relative polarity (L/B)
2
1.6
1.2
0.8
0.4
0
*
*
ns
PIN7
M3
0 min
40 min
D
Root bending angle (°)
100
80
60
40
20
0
0
2
4
6
8
10
Time interval (h)
WT
PIN7
M3PIN7
pin7

FIGURE 7. Effect of M3 mutation on PIN7 trafficking and root gravitropism .

(A) Fluorescence images of PIN7 (*ProPIN7:PIN7:GFP*) and M3PIN7 (M3, *ProPIN7:M3PIN7:GFP*) in root columella cells. Images were taken before (0 min) or after 90° −gravity stimulation for 15min. Arrows indicate the gravity direction Bar=20 μm.
(B) Fluorescence images of PIN7 and M3PIN7 in root columella regions after 40−min gravity stimulation. Arrow indicates the gravity direction. Transgenic seedlings were observed with FM4−64 staining (2 μM, within 3 min). Bar=20 μm.
(C) The lateral/basal (L/B) ratio of PIN7 or M3PIN7 fluorescence intensity in the columella cells in (B). Data represent means±SE (n=12 cells from 5 roots for each construct). Asterisks indicate that differences are significant from the PIN7 control ($P<0.0001$).
(D) Kinetics of root gravitropism of wild −type (WT), *pin7* and *pin7* complemented with PIN7, M3, and 3m1. Data represent means±SE (n=29−40 roots).

4. Discussion

After the first identification of M3 motif in PIN3-HL (Ganguly et al., 2012a), the conserved role of M3 phosphorylation site were investigated in other long PINs (PIN1, PIN2, and 7) using the root hair assay system (under *proE7*; Sasayama et al., 2013). In this study, we identified the conserved role of M3 phosphorylation site of long-looped PINs for PIN polarity and biological roles in their own expression domain. Defects in M3 site phosphorylation resulted in proper PM targeting and polarity, and subsequently caused the PIN-mediated plant developmental defects such as cotyledon development, primary stem growth, silique formation and root gravitropism defects.

The TPRXS motifs in long-looped PIN-HL were sequentially conserved in *Arabidopsis* and other orthologs, and the previous studies showed that these three TPRXS motifs in PIN-

HL have redundant function for the PIN polarity and biological functions. The M3 motif, which includes the first TPRXS motif (2m3) in the PIN-HL with RKSNASRRSF(/L) motif adjacent the 2m3 (3m1), has been studied for subcellular localization and the biological functions of PIN3 (Ganguly et al., 2102a). Our previous study demonstrated that the 3m1 mutation alone showed the partial disruption in PIN3 function but 2m3 alone did not (Ganguly et al., 2012a). Also, the root hair assay data of PIN1, 2 and 7 showed the importance of 3m1 site in PIN-HL for proper PM targeting for modulating auxin gradient formation (Sasayama et al., 2013). Consistent with that, this data revealed the decisive role of conserved M3 and 3m1site for long-PIN trafficking and biological function in their expression domain.

Protein phosphorylation and dephosphorylation is important in proper PIN trafficking and auxin transport. Subcellular localization analysis in this study revealed that the M3

site phosphorylation is crucial in proper PIN trafficking and polarity in native state or environmental stimuli. In wild-type plant, PIN1 plays pivotal role in producing reproductive organ formation such as flowers and seeds and PIN7 in columella cells plays in response to the gravity stimulation. In this study, both M3PIN1 and M3PIN7 showed disruption in proper polar targeting in their expression domain. This data suggest that the proper localization and dynamic recycling result from the M3 site phosphorylation is a crucial cue for modulating local auxin gradient in plant developmental and environmental changes.

In accordance with the root hair assay data of M3PIN2 (Sasayama et al., 2013), the phosphorylation-defective of M3 data under its own promoter also showed extremely lowered PIN2 expression which is considered because of the vacuolar lytic degradation (Data not shown). Wortmannin, an inhibitor of the vacuolar lytic pathway, treatment in M3 and 3m1 mutant showed

restored protein levels of PIN2 and this data supported the idea that the decreased protein levels shown in M3PIN2 and 3m1PIN2 are mainly due to the protein degradation (Data not shown). Unlike the M3 site analysis of PIN1 and PIN7 which showed the importance of M3 site in PM targeting or trafficking of PINs, M3PIN2 under root hair assay system (*proE7*; Sasayama et al., 2013) and under its own domain (*proPIN2*; this study) analysis showed that the M3 site phosphorylation in PIN2 plays for facilitation of vacuolar lytic pathway.

Overall, our previous data and this study suggest that the M3 motifs in long-PINs are functionally conserved in PIN trafficking, PM targeting and vacuolar lytic trafficking. In addition, after the first identification of 3m1 motif in PIN3, we investigated the function of this motif are functionally conserved in long-PINs. By comparing the different subcellular localization and trafficking of M3PINs in different cell types- and PIN-specific, we can

consider this specific expression of M3PINs can be due to evolutionary diverged function of known or unknown phosphorylation of PIN-HL among cell type- and PIN-specific manner by different AGC kinases and phosphatases.

5. LITERATURE CITED

Barbosa, I.C., and Schwechheimer, C. (2014). Dynamic control of auxin transport-dependent growth by AGCVIII protein kinases. *Curr. Opin. Plant Biol.* 22, 108-115. doi:10.1016/j.pbi.2014.09.010

Benková, E., Michniewicz, M., Sauer, M., Teichmann, T., Seifertová, D., Jürgens, G., et al. (2003). Local, efflux-dependent auxin gradients as a common module for plant organ formation. *Cell* 115, 591-602. doi:10.1016/S0092-8674(03)00924-3

Bechtold, N., and Pelletier, G. (1998). In planta Agrobacterium-mediated transformation of adult *Arabidopsis thaliana* plants by vacuum infiltration. *Methods Mol. Biol.* 82,259-266. doi: 10.1385/0-89603-391-0:259

Bennett, S.R.M., Alvarez, J., Bossinger, G. and Smyth, D.R. (1995). Morphogenesis in *pinoid* mutants of *Arabidopsis thaliana. Plant J.* 8, 505-520. doi: 10.1046/j.1365-313X.1995.8040505.x

Blilou, I., Xu, J., Wildwater, M., Willemsen, V., Paponov, I., Friml, J.,

et al. (2005). The PIN auxin efflux facilitator network controls growth and patterning in *Arabidopsis* roots. *Nature* 433, 39-44. doi: 10.1038/nature03184

Dhonukshe, P., Huang, F., Galvan-Ampudia, C. S., Mähönen, A. P., Kleine-Vehn, J., Xu, J., et al. (2010). Plasma membrane-bound AGC3 kinases phosphorylate PIN auxin carriers at TPRXS(N/S) motifs to direct apical PIN recycling. *Development* 137, 3245-3255. doi: 10.1242/dev.052456.

Ding, Z., Galván-Ampudia, C.S., Demarsy, E., Łangowski, Ł, Kleine-Vehn, J, Fan, Y,. et al. (2011). Light-mediated polarization of the PIN3 auxin transporter for the phototropic response in Arabidopsis. Nat. Cell Biol. 13, 447-452 doi: 10.1038/ncb2208

Friml, J., Benková, E., Blilou, I., Wiśniewska, J., Hamann, T., Ljung, K., et al. (2002a). AtPIN4 mediates sink-driven auxin gradients and root patterning in Arabidopsis. *Cell* 108, 661-673. doi: 10.1016/S0092-8674(02)00656-6.

Friml, J., Wiśniewska, J., Benková, E., Mendgen, K. and Palme, K. (2002b). Lateral relocation of auxin efflux regulator PIN3 mediates tropism in Arabidopsis. *Nature* 415, 806-809. doi: 10.1038/415806a

Friml, J., Vieten, A., Sauer, M., Weijers, D., Schwarz, H., Hamann, T., et al. (2003). Efflux-dependent auxin gradients establish the apical-basal axis of Arabidopsis. *Nature* 426, 147-153. doi: 10.1038/nature02085

Friml J., Yang X., Michniewicz M., Weijers D., Quint A., Tietz O., et al (2004). A PINOID dependent binary switch in apical-basal PIN polar targeting directs auxin efflux. *Science* 306, 862-865. doi: 10.1126/science.1100618

Gälweiler, L., Guan, C., Müller A., **Wisman, E., Mendgen, K., Yephremov, A., and Palme, K.** (1998). Regulation of polar auxin transport by *AtPIN1* in *Arabidopsis* vascular tissue. Science 282, 2226-2230. doi: 10.1126/science.282.5397.2226.

Ganguly, A., Lee, S.H., Cho, M., Lee, O.R., Yoo, H. and Cho, H.-T. (2010). Differential auxin-transporting activities of PIN-FORMED proteins in Arabidopsis root hair cells. *Plant Physiol.* 153, 1046-1061. doi: 10.1104/pp.110.156505

Ganguly, A., Lee, S.H. and Cho, H.-T. (2012a). Functional identification of the phosphorylation sites of Arabidopsis PIN-FORMED3 for its subcellular localization and biological role. *Plant*

J. 71, 810-823. doi: 10.1111/j.1365-313X.2012.05030.x

Ganguly, A., Sasayama, D. and Cho, H.-T. (2012b). Regulation of the polarity of protein trafficking by phosphorylation. *Mol. Cells* 33, 423-430. doi: 10.1007/s10059-012-0039-9

Ganguly, A, Park, M, Kesawat, MS and Cho, H.-T. (2014). Functional analysis of the hydrophilic loop in intracellular trafficking of Arabidopsis PIN-FORMED proteins. *Plant Cell* 26, 1576-1585. doi: 10.1105/tpc.113.118422

Grunewald, W. and Friml, J. (2010). The march of the PINs: developmental plasticity by dynamic polar targeting in plant cells. *EMBO J.* 29, 2700-2714. doi: 10.1038/emboj.2010.181

Huang, F., Zago, M.K., Abas, L., van, M.A., Galván-Ampudia, C.S. and Offringa, R. (2010). Phosphorylation of conserved PIN motifs directs Arabidopsis PIN1 polarity and auxin transport. *Plant Cell* 22, 1129-1142. doi: 10.1105/tpc.109.072678

Kleine-Vehn J., Ding Z., Jones A.R., Tasaka M., Morita M.T. and Friml J (2010). Gravity-induced PIN transcytosis for polarization of auxin fluxes in gravity-sensing root cells. *Proc. Natl. Acad. Sci.*

U.S.A. 107, 22344-22349 doi: 10.1073/pnas.1013145107

Křeček P., Skůpa P., Libus J., Naramoto S., Tejos R., Friml J. and Zažímalová E (2009). The PIN-FORMED (PIN) protein family of auxin transporters. *Genome Biol.* 10, 249. doi: 10.1186/gb-2009-10-12-249

Lee, S.H. and Cho, H.-T. (2006). PINOID positively regulates auxin efflux in Arabidopsis root hair cells and tobacco cells. *Plant Cell* 18, 1604-1616. doi: 10.1105/tpc.105.035972

Lee, O.R., Kim, S.J., Kim, H.J., Hong, J.K., Ryu, S.B., Lee, S.H., et al. (2010). Phospholipase A2 is required for PIN-FORMED protein trafficking to the plasma membrane in the Arabidopsis root. *Plant Cell*, 22, 1812-1825. doi: 10.1105/tpc.110.074211

Michniewicz, M., Zago, M. K., Abas, L., Weijers, D., Schweighofer, A., Meskiene, I., et al. (2007). Antagonistic regulation of PIN phosphorylation by PP2A and PINOID directs auxin flux. Cell 130, 1044-1056. doi: 10.1016/j.cell.2007.07.033

Müller, A., Guan, C., Gälweiler, L., Tänzler, P., Huijser, P., Marchant, A., et al. (1998). AtPIN2 defines a locus of Arabidopsis for root

gravitropism control. *EMBO J.* 17, 6903-6911. doi: 10.1093/emboj/17.23.6903

Okada, K., Ueda, J., Komaki, M.K., Bell, C.J., and Shimura, Y. (1991). Requirement of the auxin polar transport system in early stages of Arabidopsis floral bud formation. *Plant Cell* 3, 677-684. doi: 10.1105/tpc.3.7.677

Prasad, K., Grigg, S. P., Barkoulas, M., Yadav, R. K., Sanchez-Perez, G. F., Pinon, V., et al. (2011). Arabidopsis PLETHORA transcription factors control phyllotaxis. *Curr. Biol.* 21, 1123-1128. doi: 10.1016/j.cub.2011.05.009

Reinhardt, D., Pesce, E. R., Stieger, P., Mandel, T., Baltensperger, K., Bennett, M., Traas, J., Friml, J. and Kuhlemeier, C. (2003). Regulation of phyllotaxis by polar auxin transport. *Nature* 426, 255-260. doi: 10.1038/nature02081

Sasayama, D., Ganguly, A., Park, M. and Cho, H.-T. (2013). The M3 phosphorylation motif has been functionally conserved for intracellular trafficking of long-looped PIN-FORMEDs in the Arabidopsis root hair cell. *BMC Plant Biol.* 13, 189. doi: 10.1186/1471-2229-13-189

Wiśniewska J., Xu J., Seifertová D., Brewer P.B., Ruzicka K., Blilou I., Rouquié D., Benková E., Scheres B. and Friml J. (2006). Polar PIN localization directs auxin flow in plants. *Science* 312, 883. doi: 10.1126/science.1121356

Zhang Y. and McCormick S. (2008). AGCVIII kinases at the crossroads of cellular signaling. *Trends Plant Sci.* 14, 689-695. doi: 10.1016/j.tplants.2009.09.006

Zourelidou M, Absmanner B, Weller B, Barbosa IC, Willige BC, Fastner A, Streit V, Port SA, Colcombet J, de la Fuente van Bentem S et al. (2014) Auxin efflux by PIN-FORMED proteins is activated by two different protein kinases, D6 PROTEIN KINASE and PINOID. *Elife* 19, 3. doi: 10.7554/eLife.02860

6. ABSTRACT IN KOREAN

M3 인산화 부위가 PIN-FORMED 옥신수송체의 세포 내 수송 및 애기장대의 발달에 미치는 영향

기 대 은

서 울 대 학 교 대 학 원

생 명 과 학 부

비대칭적으로 위치하는 옥신 수송체 단백질인 PIN은 세포간 옥신의 이동과 이로 인한 옥신 gradient 형성에 중요한 역할을 한다. PIN의 central hydrophilic loop (HL)에서의 인산화는 PIN의 극성 분포에 중요한 역할을 한다고 여겨지며, PIN-HL의 RKSNASRRSF(/L)와 TPRPSNL 모티프에 위치하는 M3 인산화 site는 PIN3에서 그 중요성이 밝혀졌다. 본 연구에서, 우리는 M3 인산화 site의 보존된 역할을 애기장대 PIN1와 PIN7을 통해서 분석 해 보았다. M3 site에 위치하는 인산화

가능한 5개의 residue의 phosphorylation-defective mutation (Ser/Thr to Ala or Gly)을 통해 연구 해 보았을 때, PIN1-HL의 M3 site mutation은 PIN1의 subcellular localization의 변화와 그로 인한 뿌리 성장, 로제트 잎의 phyllotaxy, floral organ 형성 등에 영향을 끼쳤다. 또한, PIN7-HL의 M3 site mutation은 root columella cell에서의 PIN7 단백질의 trafficking 변화를 야기했으며, 이로 인한 root gravitropism defect가 관찰되었다. 종합적으로, 우리의 분석은 M3 인산화 site가 long-looped PIN 간에 기능적으로 보존되어 있으며, PIN의 subcellular trafficking, 옥신 분포 그리고 옥신에 의해 야기되는 애기장대 발달과정에 중요한 역할을 한다고 판단된다.

.....

핵심어: PIN, 옥신, 옥신 수송, 인산화, 단백질 trafficking
학번: 2014-21269